Theoretical Study of Syndiospecific Styrene Polymerization with Cp-Based and Cp-Free Titanium Catalysts. 1. Mechanism of Chain Propagation

Gianluca Minieri,† Paolo Corradini,† Adolfo Zambelli,‡ Gaetano Guerra,‡ and Luigi Cavallo†*

Dipartimento di Chimica, Università di Napoli Federico II, Complesso Monte S. Angelo, Via Cintia, I-80126, Napoli, Italy; and Dipartimento di Chimica, Università di Salerno, Via S. Allende, Baronissi (SA), I-84081, Italy

Received December 20, 2000

ABSTRACT: A theoretical study of the mechanism of styrene polymerization with models based on the $CpTiP^+$ (P = polymeryl) species is presented. The styrene-free $CpTiCH_2Ph^+$ species, with a coordinated benzene molecule to simulate the solvent, is characterized by two minimum geometries with different hapticities of coordination of the benzyl group. The η^3 coordination is more stable than the η^7 coordination by 12 kJ mol^{-1}. Substitution of the solvent molecule by styrene leads to coordination intermediates which are also characterized by different hapticities of the styrene. When the benzyl group is η^7 coordinated the styrene is η^2 coordinated, while in the case of η^3 coordination of the benzyl group, styrene is η^4 coordinated. All these coordination intermediates are of similar energy and are separated by low energy barriers. Insertion can occur with a relatively small energy barrier, 47 kJ mol^{-1}, from a coordination intermediate presenting a η^3 coordinated growing chain, and a η^4-coordinated styrene molecule. The products of the insertion reaction are characterized by a backbiting of the aromatic ring of the penultimate unit. As for the role of Ti^{II} active species, our calculations suggest that neutral active species of the type $CpTi^{II}P$ should be not able to promote styrene polymerization, whereas cationic active species of the type (benzene)$Ti^{II}P^+$ should be able to promote styrene polymerization, although the latter species should be less active than species of the type $CpTi^{III}P^+$.

Introduction

Syndiotactic polystyrene is a new polymeric material of industrial relevance.[1−6] Despite the complex polymorphic behavior,[7] the high crystallization rate and the high melting point, 270 °C,[8] make syndiotactic polystyrene a crystalline engineering thermoplastic material with potential applications. Syndiotactic polystyrene is currently being commercialized by Dow Chemical Co. and by Idemitsu Petrochemical Co., Ltd., under the trade names Questra and XAREC, respectively. First discovered in 1986 by Ishihara and co-workers,[8,9] syndiotactic polystyrene is a highly stereoregular polymer (fraction of the *rrrrrr* heptad >94%)[9] which can be obtained with several soluble titanium and, to a lesser extent, zirconium compounds.[10]

The best performances are obtained with monocyclopentadienyl compounds of titanium, such as $CpTiX_3$ or Cp^*TiX_3 (Cp = η^5-C_5H_5, Cp* = η^5-C_5Me_5 or another substituted Cp ligand, X = F, Cl)[11−17] activated by methylalumoxane (MAO) or $B(C_6F_5)_3$.[18,19] Cp-free compounds as $Ti(CH_2Ph)_4$, $Ti(OR)_4$ (R = alkyl, aryl) are also moderately active.[20] In short, many soluble titanium compounds can be used as precatalyst, but it is worthwhile to note that titanocene compounds, quite active in the polymerization of 1-olefins,[21] are among the less active species for styrene polymerization,[9,22] and that zirconium compounds are generally much less active than the analogous titanium compound.[10]

The nature of the real active species in styrene syndiotactic polymerization is still debated in the literature.[23−32] On the basis of kinetic, ESR, and NMR studies, Zambelli and co-workers proposed that the real active species could be of the type $CpTi^{III}P^+$ (P = polymeryl), for the Cp-based systems, and of the type (arene)$Ti^{II}P^+$ for the Cp-free systems. In the latter case, the Cp ring would be replaced by an arene neutral η^6-ligand, affording a cationic Ti^{II} complex.[33−36] NMR monitoring of the reaction of Cp^*TiR_3 (R = CH_3, CH_2-Ph) with $B(C_6F_5)_3$ showed the formation of the ionic compound $[Cp^*TiR_3^+][B(C_6F_5)_3^-]$, although about 25% of the total titanium was not NMR detectable.[25,27] Addition of styrene resulted in the formation of syndiotactic polystyrene, while the Ti^{IV} spectrum was not affected, suggesting that the latter does not take part to the active species. ESR studies of the same system indicated that Ti^{III} species were formed, although attempts to isolate them were unsuccessful.[27,28] Moreover, in situ ESR monitoring of the *p*-chlorostyrene polymerization with the above-mentioned $Cp^*TiR_3/B(C_6F_5)_3$ system, suggested that the concentration of active species were similar to Ti^{III} concentration. Addition of α-^{13}C-*p*-chlorostyrene to the ESR tube resulted in the ESR signal showing ^{13}C coupling, indicative of a Ti^{III}−^{13}C bonding.[30]

Although the above results seem quite convincing, there are other studies which suggest that species other than $Cp^*Ti^{III}P^+$ could be involved in the polymerization reaction. Chien and co-workers noticed a considerable reduction of titanium in Cp^*TiMe_3/MAO to lower oxidation states, but no ESR signals were observed.[26] Moreover, the activities of a series of indenyl-substitued titanium/MAO compounds indicated that the compounds which were the most active were also the less prone to undergo reduction.[37] Finally, ESR and NMR

* Corresponding author. E-mail: cavallo@chemistry.unina.it.
† Università di Napoli Federico II.
‡ Università di Salerno.

10.1021/ma002162l CCC: $20.00
Published on Web 03/17/2001

studies of Cp*$TiMe_3$ and Cp*$TiCl_n$ ($n = 2, 3$) performed by Baird and co-workers have indicated that Ti in the oxidation states II, III, and IV can be present and that the putative active Cp*$TiMe^+$ species should be less than 10% of the total amount of titanium. They also suggested that reaction of titanium compound precursors with MAO could lead to formation of species of the type $CpTiMe_2$, which could undergo disproportion to titanium II products which might be catalytically active.[25,32,38] Finally, the proposal that Ti(IV) species could be active in syndiotactic polymerization is hardly supported by the low activity of that titanocene compounds[9,22] and by the fact that the few zirconocenes active in styrene and styrene/ethene copolymerizations usually lead to highly isotactic polymers.[39,40] In conclusion, a definitive experimental proof that a species of the type $CpTi^{III}P^+$ is active in the syndiospecific styrene polymerization is still missing, although it remains by far the most plausible.

Although there is some debate about the exact nature of the species active in polymerization, many characteristics of the polymerization mechanism have been addressed beyond any doubt. NMR experiments have clearly indicated that polymerization of styrene to syndiotactic polymer occurs through a Ziegler−Natta type polyinsertion mechanism. In particular, these experiments have shown the following. (i) The insertion occurs through cis opening of the monomer double bond, as indicated by the ^{1}H NMR analysis of the random copolymers of perdeuteriostyrene with low amounts of *Z*-1-d_1-styrene.[41] (ii) The regiochemistry of styrene insertion is secondary, since the ^{13}C NMR analysis of the end groups of polystyrene samples prepared in the presence of ^{13}C enriched $AlEt_3$ showed the presence of the $-CH(Ph)CH_2{}^{13}CH_2CH_3$ end groups.[42] Moreover, in the NMR analysis of polystyrene samples of low molecular weight, only the $-CH(Ph)CH_3$ and $PhCH{=}CH_2-$ end groups were observed.[43] Both are indicative of secondary insertion in the initiation and termination steps. Finally, the substantial absence of regioirregular head-to-head and tail-to-tail sequences in the body of the polymer is indicative that propagation occurs with almost perfect regioselectivity. (iii) The stereoselectivity of the insertion step is controlled by the chirality of the growing-chain end. This is clearly indicated by the analysis of the stereochemical composition of the syndiotactic polymers, which shows the presence of *rmr* tetrads, which is consistent with a chain-end stereocontrol, and the substantial absence of *rmm* tetrads, which would be consistent with a site-stereocontrol.[10,35,44,45]

While many experimental studies have provided substantial information on the polymerization mechanism, up to now almost nothing has been done from a theoretical point of view. This is in sharp contrast to the considerable amount of high level computational studies which have contributed to the comprehension of fine details of olefins polymerizations with both early and late transition metals.[46−48] For these reasons, we decided to make a density functional study of the elementary steps which compose the propagation cycle. In particular, we have investigated coordination and insertion of styrene on the $CpTi^{III}CH_2Ph^+$ active species, in which the achiral $-CH_2Ph$ group has been used to simulate the growing chain. This choice allowed us to explore the elementary steps of the insertion reaction delaying the complicacies due to the presence of a chiral growing chain. Moreover, we also investigated styrene insertion on the neutral and cationic $CpTi^{II}CH_2Ph$ and $(C_6H_6)Ti^{II}CH_2Ph^+$ species, to have insights on the possible role of active species with different titanium oxidaton states. The issue of syndiospecific chain-end stereocontrol, which also is relevant, will be considered in a different paper.[49] We only anticipate that the most favored transition state of the insertion step, reported in this paper, will be the key structure to rationalize the syndiospecific behavior of these catalysts. Finally, since the scope of this paper is an investigation of species possibly active in the syndiospecific styrene polymerization, Ti(IV) species have been not considered.

Computational Details

Stationary points on the potential energy surface were calculated with the Amsterdam Density Functional (ADF) program system, release 2.3.0,[50] developed by Baerends et al.[51−54] The electronic configuration of the molecular systems were described by a triple-ζ basis set on titanium for 3s, 3p, 3d, and 4s, plus one 4p function (ADF basis set IV).[50] Double-ζ STO basis sets were used for carbon (2s, 2p) and hydrogen (1s), augmented with a single 3d and 2p function, respectively (ADF basis set III).[50] The inner shells on titanium (including 2p) and carbon (1s) were treated within the frozen core approximation. Energetics and geometries were evaluated by using the local exchange-correlation potential by Vosko et al.,[55] augmented in a self-consistent manner with Becke's exchange gradient correction[56] and Perdew's correlation gradient correction.[57,58] An unrestricted formalism was used for all species with unpaired electrons. The energy differences with inclusion of solvent effects were calculated by correcting the gas-phase energy with the use of the conductor-like screening model, COSMO, of Klamt and Schüürmann,[59] as implemented in the ADF package.[60] The calculations of the solvation energy were performed with a dielectric costant of 2.38 to represent toluene as solvent. The van deer Waals surface was used to build the cavity containing the molecule, and the standard radii H = 1.29 Å and C = 2.00 Å, of Klamt and Schüürmann were used.[59] For Ti, we used a radius of 2.30 Å, as proposed by Ziegler and co-workers.[61] The calculations of energies including solvation effects were performed as single point calculations on the gas-phase optimized geometries. The 2000.01 release of the ADF package was used for these calculations.[62]

Results and Discussion

(1) Monomer-Free Species. The definition of the structure of the monomer-free intermediates, that is of the catalytic complexes at the beginning of each insertion step, is relevant for evaluation of monomer coordination energies and hence for location of possible coordination intermediates as well as for evaluation of energy barriers for insertion reactions. The monomer-free intermediates usually assumed for olefin polymerizations by insertion catalysts, present only the growing chain bonded to the metal, beside stable ligands. For this kind of intermediates the addition of a monomer to the metal coordination sphere

$$\text{catalyst(chain)} + \text{monomer} \rightarrow \text{catalyst(chain)(monomer)}$$

involves entropy contributions to the free energies of coordination which substantially counterbalance and sometime overcome the attractive enthalpic contributions. Entropy contributions of the order of 40−60 kJ/mol ($T\Delta S$ at 298 K) have been measured[63] or calculated[64,65] for ethene coordination to similar catalyst systems. It is worth noting that these significant entropy contributions generally are not accounted for in modeling studies relative to insertion polymerization catalysis.

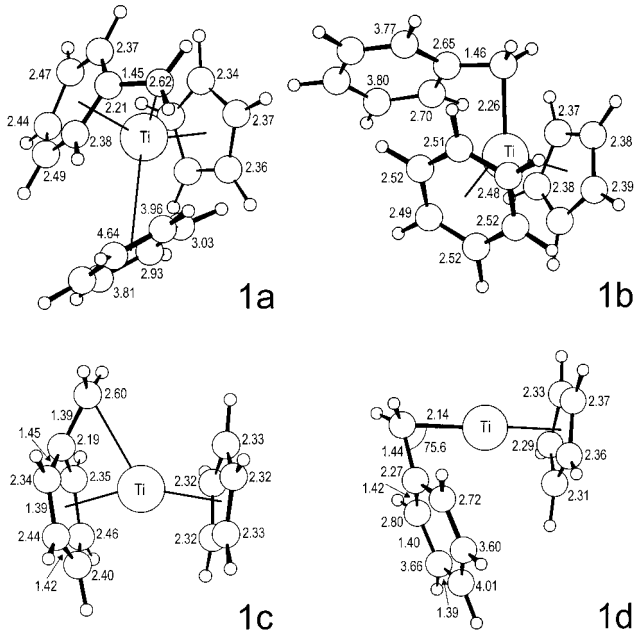

Figure 1. Minimized energy geometries of the benzene coordinated and of the naked $CpTiCH_2Ph^+$ species. The numbers close to the C atoms represent the distance of these atoms from the metal. All distances are reported in Å.

As in previous studies,[66,67] we here consider models of monomer-free intermediates which also present a benzene molecule (to simulate the solvent) coordinated to the metal. Of course, in this assumption the monomer coordination implies a solvent molecule substitution reaction in the metal coordination sphere

$$\text{catalyst(chain)(solvent)} + \text{monomer} \rightarrow \text{catalyst(chain)(monomer)} + \text{solvent}$$

this way, the entropy changes along the insertion paths are reduced, thus making more reasonable the usual simplifying assumption to ignore the coordination entropy.

The most stable structures of $CpTiCH_2Ph^+$ with a benzene molecule coordinated are **1a** and **1b** of Figure 1. In structure **1a** the benzyl group coordinates to the metal with all the C atoms of the aromatic ring, as suggested by the short (<2.5 Å) Ti−C(phenyl) distances. The distance between the C atom of the CH_2 group and the Ti atom, 2.62 Å, is considerably longer than standard Ti−C σ-bond distances, which are close to 2.15−2.20 Å, usually.[68] Moreover, the C(phenyl)−CH_2 distance is considerably shorter than a sp^2-sp^3 C−C bond distance, which suggests a strong double bond character for this bond. Finally, the phenyl ring is distorted toward a boatlike conformation. The benzene molecule, instead, is substantially η^2 coordinated, since two C atoms only are at distance of interaction from the Ti atom. The overall geometry of **1a** reminds of a metallocene structure in which one of the Cp rings is replaced by the phenyl ring of the benzyl group, which is η^7 coordinated to the metal. The angle between the centroids of the Cp and of the phenyl rings is 147.5°. The geometry of coordination of the benzyl group in **1a** is very similar to the geometry of coordination of one of the benzyl groups (the one which is η^7 coordinated) in the X-ray structure of the $[Cp^*Zr(CH_2Ph)_2]^+[B(CH_2Ph)C_6F_5)_3]^-$ ionic complex. The molecular orbital analysis we performed on the bonding of the benzyl group to the Ti atom is in total agreement with the extended Huckel analysis performed by Pellecchia and Peluso.[69]

Structure **1b**, in a different manner, presents a substantial interaction between the C atom of the benzyl CH_2 group and the Ti atom. The Ti−CH_2 bond distance, 2.14 Å, is in the range usually observed for Ti−C σ-bond distances.[68] Moreover, the phenyl group is strongly bent toward the Ti atom, and an interaction between the *ipso*-C atom, and the Ti atom exists. The substantial η^3 coordination of the benzyl group is quite similar to the way of coordination of the benzyl groups in the X-ray structure of the $Ti(CH_2Ph)_4$ complex.[70] The benzene molecule, instead, is substantially η^6 coordinated to the metal, as suggested by the short (∼2.5 Å) Ti−C(benzene) distances. From an energetical point of view, structure **1b** is favored relative to structure **1a** by 12 kJ mol^{-1} only.

In the absence of the benzene molecule, the naked $CpTiCH_2Ph^+$ structure with a η^7-coordinated growing chain **1c**, is favored with respect to the naked structure with a η^3-coordinated growing chain **1d**, by 51 kJ mol^{-1}. The greater stability of **1c** with respect to **1d** is clearly due to the η^7 coordination of the benzyl-type growing chain, which reduces the electron deficiency at the metal atom. The benzene uptake energy to **1c** and **1d**, to lead to the solvent coordinated **1a** and **1b** structures, is 49 and 110 kJ mol^{-1}, respectively.

(2) Monomer-Coordinated Species. As for monomer coordination to structures **1a** and **1b**, after removal of the benzene molecule, we restricted our analysis to styrene approaches leading to situations suitable for secondary insertion, due to the high regiospecificity experimentally observed in the polymerization of styrene with these catalytic systems.[43] Results regarding the regiospecificity of styrene insertion will be reported elsewhere.

Styrene coordination to **1a** leads to structures **2a** and **2b** of Figure 2. They substantially differ for the relative orientation of the Cp ring and of the styrene phenyl group. In structure **2a**, they are on opposite sides (i.e., anti) of the plane defined by the Ti atom and by the two C atoms of the styrene double bond, whereas in structure **2b**, they are on the same side (i.e., syn). Independently of the relative orientation of these two groups, the styrene η^2 coordinates to the Ti atom. In fact, in both **2a** and **2b** the C atoms of the styrene double bond are at distances of coordination from the Ti atom (smaller than 2.7 Å), whereas the shortest Ti−C distance involving a C atom of the styrene phenyl group is longer than 3.5 Å. Finally, both in **2a** and **2b** the benzyl group preserves a η^7 coordination very similar to that of structure **1a**. As for the relative stability, **2a** and **2b** are almost isoenergetic, with structure **2a** favored by 4 kJ mol^{-1} only, while the displacement of the solvent molecule with a styrene molecule from **1a** to **2a** is exothermic by 38 kJ mol^{-1}.

Styrene coordination to **1b** lead to structures **2c**−**f** of Figure 2. Structures **2c** and **2e**, present the same relative anti orientation of the Cp ring and of the styrene phenyl group as in **2a**, while in structures **2d** and **2f**, these two groups are syn oriented as in **2b**. In **2c**−**f** the styrene coordinates to the Ti atom in a η^4 fashion. Moreover, in **2c** and **2d** the styrene is *trans*-coordinated, while in **2e** and **2f** it is *cis*-coordinated. In the **2c**−**f** structures, the aromatic ring of the benzyl group is slightly farther from the Ti atom, relative to **1b**, to accommodate the coordinated styrene molecule.

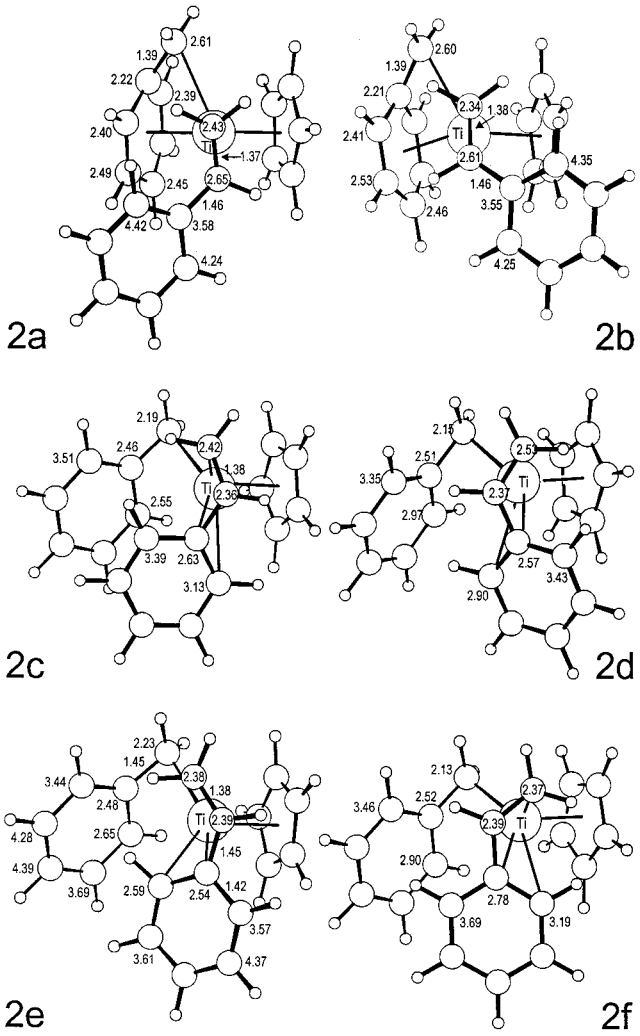

Figure 2. Minimized energy geometries of the coordination intermediates obtained by styrene coordination to the $CpTiCH_2$-Ph^+ species. The numbers close to the C atoms represent the distance of these atoms from the metal. All distances are reported in Å.

From an energetical point of view, structures **2c**−**f** are less stable of **2a** by 18, 15, 15, and 26 kJ mol^{-1}, respectively.

Considering that species **2a**−**f** are of quite similar energy, independently of the hapticity of coordination of either the benzyl group and of the styrene, we investigated possible rearrangements which could connect structures with different hapticity and/or orientation of the ligands. As examples, we report the transition states for interconversion between the most stable coordination intermediate **2a**, and structures **2c** and **2e**, all of them with a relative anti orientation of the Cp ring and of the styrene phenyl group. Forcing the aromatic ring of the benzyl group away from the metal, we localized the transition state between **2a** and **2c**, **TS[2a**−**c]** of Figure 3. The latter substantially corresponds to the transition state of a ligand substitution reaction in which the aromatic ring of the benzyl group is displaced from the coordination sphere of the Ti atom by the aromatic group of the styrene. As the aromatic ring of the benzyl group moves away from the metal, the CH_2 group of the benzyl group moves toward the Ti atom giving rise to the Ti−C σ-bond characterizing structures **1b** and **2c**−**f**. At the same time, the styrene molecule slips over the Ti atom, with an increase in the

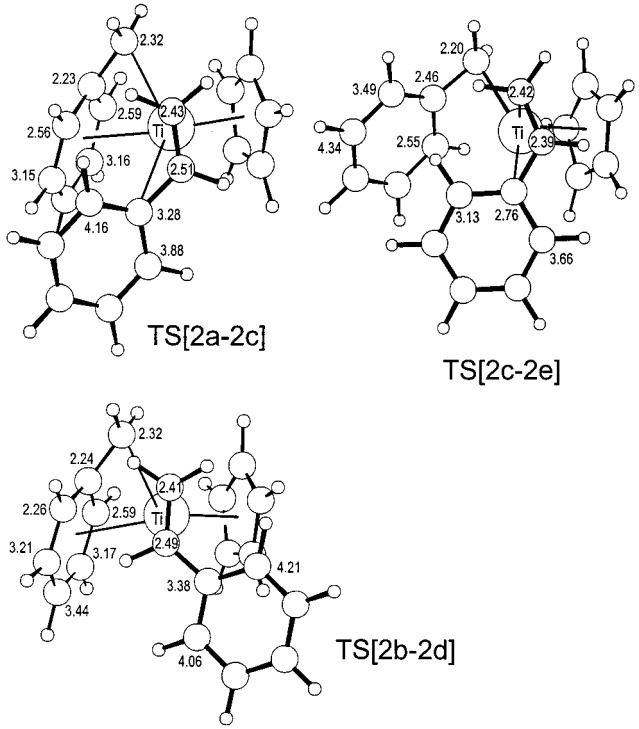

Figure 3. Geometries of the transition states for interconversion between different coordination intermediates. The numbers close to the C atoms represent the distance of these atoms from the metal. All distances are reported in Å.

hapticity of coordination. The relatively small energetic barrier for the conformational rearrangement **2a** → **2c** amounts to 28 kJ mol^{-1}. With regards to the interconversion between structures **2c** and **2e**, which are characterized by trans- and cis-coordinated styrene, respectively, we localized the transition state **TS[2c**−**e]** of Figure 3. This interconversion requires a small rotation of 30° around the CH_2CH−C(phenyl) bond, and the overcome of a barrier of 9 kJ mol^{-1}, only. As for interconversion between structures **2b**, **2d**, and **2f**, we focused our attention on the **2b** → **2d** rearrangement only, since it modifies more the coordination scheme around the metal atom. The transition state, **TS[2b**−**d]** of Figure 3 and the energetic barrier (30 kJ mol^{-1}) for this interconversion are quite similar to those of the analogous interconversion **2a** → **2c**.

The small barriers which separate low energy coordination intermediates with different hapticity and geometry of coordination of the benzyl group and of the styrene, are in agreement with the fluxional behavior experimentally shown by the $[Cp^*Zr(CH_2Ph)_2]^+[B(CH_2Ph)C_6F_5)_3]^-$ complex.[69] Moreover, in the following discussion which is concerned with the insertion step, structure **2a** will be the reference state at 0 kJ mol^{-1}, since it is reasonable to assume a rapid interconversion between the coordination intermediates.

(3) Transition States for the Insertion Reaction. With regards to monomer insertion into the Ti−CH_2-(benzyl) bond, we investigated reaction paths which could start from **2a** and **2b**, with the styrene molecule η^2-coordinated, as well as from **2e** and **2d**, which are the most stable species with a styrene molecule η^4-coordinated. Coordination intermediates **2a** and **2e** will lead to transition states featuring an anti orientation of the styrene aromatic group and of the Cp ring, while in the transition states reached from **2b** and **2d**, these groups will present a relative syn disposition.

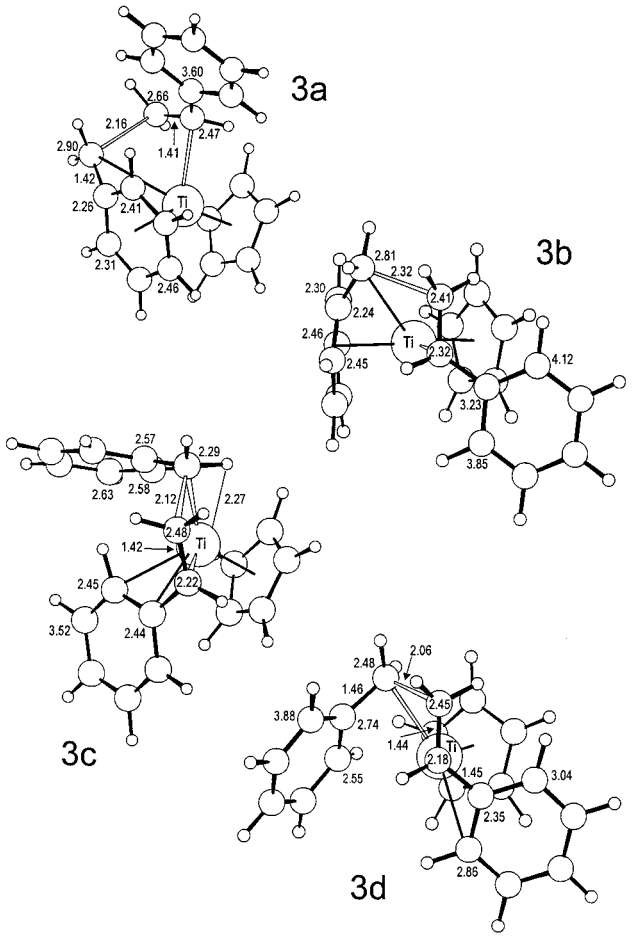

Figure 4. Geometries of the transition states for insertion of styrene on the $CpTiCH_2Ph^+$ species. The numbers close to the C atoms represent the distance of these atoms from the metal. All distances are reported in Å.

Starting from structure **2a**, with the styrene η^2-coordinated and with a relative anti orientation of the Cp ring and of the styrene phenyl group, we shrunk the distance between the C atom of the CH_2 groups of styrene and of the benzyl group. This way, we localized the transition state **3a** of Figure 4, which does not presents the classical planar four-centers transition state which is characteristic of 1-olefins polymerization reactions. In fact, the torsional angle Ti−CH(styrene)−CH_2(styrene)−CH_2(benzyl) assumes a value close to 60°. Moreover, **3a** shows a very long distance between the Ti atom and the C atom of the benzyl CH_2 group, a feature already present in **2a**. The forming C−C bond has a value of 2.16 Å, which is in line with the analogous distance in the transition states for olefin polymerization by group 4 metallocenes.[71] Energetically, **3a** lies 77 kJ mol^{-1} above **2a**. This high energy barrier substantially stems from the absence of stabilizing interactions between d orbitals of the metal with one of the sp^3 orbitals of the C atom of the benzyl CH_2 group, due to the unfavorable distance and orientation of these two atoms. Similar calculations using as starting point the intermediate **2b**, with the styrene η^2-coordinated and with a relative syn orientation of the Cp ring and of the styrene phenyl group, lead to a quite similar situation. The so localized transition state, **3b** of Figure 4, is even of higher energy, 102 kJ mol^{-1} above **2b**, due to repulsive steric interactions between the styrene aromatic ring and the Cp ring, which are now in a relative syn disposition.

Starting from **2e**, with the styrene cis-η^4-coordinated and with a relative anti orientation of the Cp ring and of the styrene phenyl group, the transition state **3c** of Figure 4 was found, which presents the classical four centers geometry characterizing olefins polymerization reactions. The Ti−CH_2(benzyl), Ti−CH(styrene), and CH_2(styrene)−CH_2(benzyl) distances are very close to the analogous distances in the transition states for olefin polymerization with group 4 metallocenes. The torsional angle Ti−CH(styrene)−CH_2(styrene)−CH_2(benzyl) assumes a value close to −8°, which indicates an almost planar transition state geometry. Moreover, an adjuvant α-agostic interaction of the Ti atom with a H atom of the benzyl CH_2 groups is present. This agostic interaction is missing in the coordination intermediates **2c** and **2e**. Finally, the aromatic rings of the benzyl group and of the styrene molecule are slightly farther and closer to the Ti atom in **3c** relative to **2e**, respectively. It is worthwhile to note that approach of the styrene aromatic ring to the Ti atom occurs in a relatively uncrowded sector, due to the anti disposition of this group and of the Cp ring.

Energetically, **3c** lies 47 kJ mol^{-1} above **2a**. This barrier is higher than the insertion barrier for olefin polymerization with group 4 cationic metallocenes, which are in the range 0−20 kJ mol^{-1} when calculated with the same theoretical approach,[46,71,72] but it is in good agreement with the ethene insertion barrier (59 kJ mol^{-1}) in the $Ti(NH_3)(NH_2)^+$ species, which is cationic and d^1 as the species considered in this paper,[73] as well as with the slow chain propagation experimentally observed for styrene polymerization.[74]

For the last approach to the transition state for the insertion reaction we used as starting point **2d**, with the styrene trans-η^4-coordinated and with a relative syn orientation of the Cp ring and of the styrene phenyl group. As the distance between the C atoms which will form the new C−C bond was reduced, steric repulsions between the styrene aromatic ring and the Cp ring were observed, due to the relative syn orientation of these two groups. The transition state **3d** of Figure 4, presents the classical four centers geometry, and the Ti−C and C−C distances are quite similar to the corresponding distances in **3c**. However, to relieve the aforementioned steric stress, a strong deviation from planarity is observed in the four centers transtition state geometry. In fact, the torsional angle Ti−CH(styrene)−CH_2-(styrene)−CH_2(benzyl) assumes a value close to 46°. This deviation from planarity, and the steric stress between the monomer and the Cp ring strongly destabilize the transition state, which lies 101 kJ mol^{-1} above **2a**.

(4) Products of the Insertion Reaction. Optimizing the most favored transition state **3c** on the products side, we arrived at structure **4a** of Figure 5, which represents the kinetic product of the insertion reaction. The inserted styrene molecule evolved into the benzyl-type −CH(Ph)P (P = polymeryl) group which represents the end of the growing chain bonded to the metal. The bonding between the new benzyl-type chain-end and the metal atom is very similar to that of **1b**. In fact, the short distance between the once olefinic C atom of the CH group of styrene and the metal (2.21 Å) indicates a strong σ-bond interaction. The aromatic group of the penultimate unit is backbitten to the metal atom, since it has some C atoms at distance of coordination. Finally,

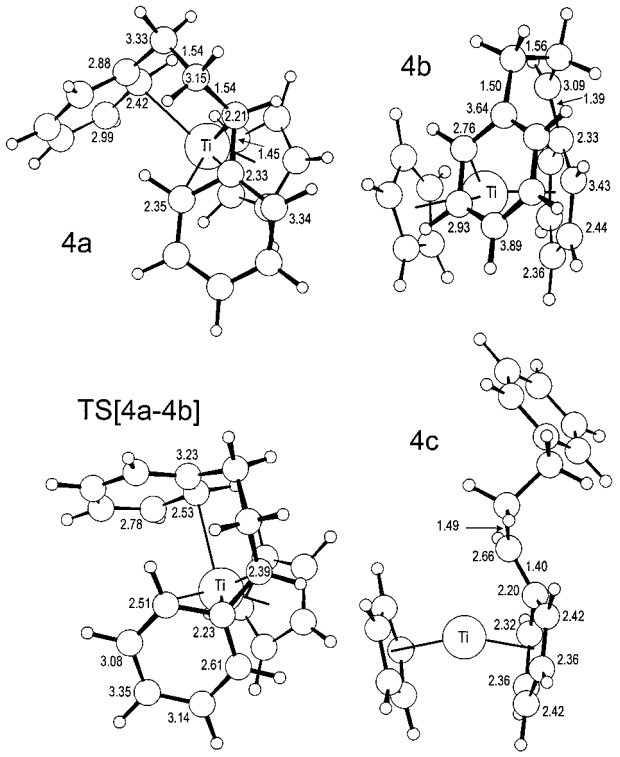

Figure 5. Minimized energy geometries of the products of the insertion of styrene on the $CpTiCH_2Ph^+$ species. The numbers close to the C atoms represent the distance of these atoms from the metal. All distances are reported in Å.

the α-agostic interaction of **3c** turned into a γ-agostic one.

However, **4a** can rearrange to the thermodynamic product **4b** of Figure 5.[75] The final product **4b** presents a η^7 coordination scheme between the metal atom and the benzyl-type chain-end very similar to that of structure **1a**. A backbiting of the aromatic ring of the penultimate unit characterizes **4b** also. The benzyl-type group coordinates to the metal with all the C atoms of the aromatic ring, and the overall structure is quite similar to a metallocene with a benzene molecule (the aromatic group of the penultimate unit) coordinated to the metal through two C atoms.[67] In this case, the benzene molecule is thetered to the six-membered aromatic ring which replaces a Cp ring of a metallocene, through the $-CHPCH_2CH-$ (P = polymeryl) spacer. The transition state which connects **4a** and **4b**, **TS[4a−b]** of Figure 5, presents a coordination scheme of the benzyl-type chain-end very similar to that of **TS[2a−c]**.

Energetically, **4a** and **4b** lie 6 and 44 kJ mol^{-1} below **2a**, respectively. The energy barrier to the rearrangement **4a** → **4b** amounts to 11 kJ mol^{-1} only. Finally, we pushed the aromatic ring of the backbitten penultimate unit far from the metal atom, and we arrived to structure **4c**. This last structure is 32 kJ mol^{-1} above **4b**, and this number can be taken as an approximation to the backbiting energy.

(5) Discussion. The energy profile of the whole reaction path for structures with a relative anti orientation of the styrene phenyl group and of the Cp ring is reported in Figure 6. All the energy values are collected in Table 1. Starting from the most stable monomer-free species **1b**, the first step of the reaction corresponds to the solvent substitution reaction by the monomer to arrive to the most stable coordination intermediate **2a**,

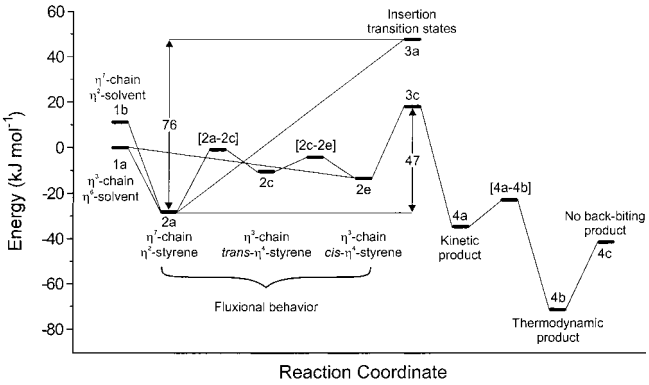

Figure 6. Energy profile of the complete path of the propagation reaction corresponding to styrene coordination and insertion on the $CpTiCH_2Ph^+$ species.

with the styrene molecule η^2-coordinated. This species is not suitable for monomer insertion, due to the relatively high energy barrier (77 kJ mol^{-1}) which has to be overcome to reach the transition state **3a**.

An alternative path can proceed through conformational rearrangements within the coordination sphere of the metal atom, which lead to the coordination intermediates **2c** and **2e**, with the styrene molecule η^4-coordinated. The highest energy barrier for this conformational rearrangement (28 kJ mol^{-1}) corresponds to the conversion of **2a** into **2c**. The coordination intermediate **2e** is particularly prone to undergo monomer insertion through the transition state **3c**, and with a relatively low energy barrier, calculated with respect to the most stable coordination intermediate **2a**, 47 kJ mol^{-1}, which slightly overestimate the experimentally determined apparent activation energy of styrene polymerization, 32 kJ mol^{-1}, using the $CpTiCl_3$/MAO catalyst.[9] The transition state **3c** then collapses into the product **4a**, which presents a η^3 interaction between the new benzyl-type chain-end and the metal atom very similar to that of **1a**. However, **4a** only is the kinetic product which can collapse through the transition state **TS[4a−b]** into the thermodynamic product **4b**, which lies 44 kJ mol^{-1} below **2a**, and presents a η^7 coordination scheme between the benzyl-type chain-end and the metal atom very similar to that of **1b**. In both the kinetic and thermodynamic products, the aromatic ring of the penultimate monomeric unit is backbitten to the metal. This backbiting should be not a hinder for the coordination/insertion of a new monomeric unit, since the backbiting energy amounts to roughly 32 kJ mol^{-1}, only. However, if coordination of a new monomeric unit occurs on the kinetic product, the coordination intermediate which would form could undergo the insertion reaction without any rearrangement, since it would present the same coordination scheme of structure **2c**.

With regards to reaction paths comprising models with a relative syn orientation of the styrene phenyl group and of the Cp ring, are characterized by transition states for the insertion step of high energy. The inaptitude of such structures to give the insertion reaction substantially stems from repulsive interactions between the Cp ring and the styrene aromatic ring, which are in a relative syn disposition.

In this final section, we report about the influence of solvent effects on the reaction path. To this end, the relative energy values in solution (see Computational Details) of all the structures without a benzene molecule coordinated to the metal, are reported in Table 1. As

Table 1. Relative Energies of the Most Relevant Structures along the Reaction Path

species	label	ΔE(g)[a]	ΔE(s)[b]	ΔE(s) − ΔE(g)
η^7-chain, + free monomer	**1c**	0	0	0
η^3-chain, + free monomer	**1d**	51	47	−4
η^7-chain, η^2-monomer	**2a**	−89	−78	11
TS for the **2a** to **2c** rearrangement	**TS[2a−c]**	−61	−50	11
σ-chain, *trans*-η^4-monomer	**2c**	−71	−58	13
TS for the **2c** to **2e** rearrangement	**TS[2c−e]**	−65	−53	12
σ-chain, *cis*-η^4-monomer	**2e**	−74	−60	14
insertion TS with η^7-chain, η^2-monomer	**3a**	−12	−4	8
insertion TS with σ-chain, η^4-monomer	**3c**	−42	−29	13
kinetic product	**4a**	−95	−78	17
TS for the **2c** to **2e** rearrangement	**TS[4a−b]**	−84	−68	16
thermodynamic product	**4b**	−133	−116	17
no back-biting product	**4c**	−101	−93	8

[a] Gas-phase energy with respect to that of **1c** plus a free styrene molecule. [b] Energy values in solution (see methods) with respect to that of **1c** plus a free styrene molecule.

expected, inclusion of solvent effects reduces considerably, by 11 kJ mol^{-1}, the styrene uptake energy. Nevertheless, even including solvent effects the styrene uptake energy, 78 kJ mol^{-1}, is high enough to counterbalance the unfavorable $-T\Delta S$ contribution which can be roughly estimated to be close to 40 kJ mol^{-1}.[76]

As for the remaning part of the reaction path, solvent effects play a minor role, since all the structures are stabilized similarly. The major effcts are on the products of the insertion reaction, which are slightly less stabilized than the other structures. The overall energy gain from the most stable coordination intermediate **2a**, to the thermodynamic product **4b**, decreases from 44 kJ mol^{-1} in the gas phase, to 38 kJ mol^{-1} when solvent effects are considered. Finally, it is also reasonable that solvent effects reduces the relevance of the backbiting of the penultimate unit in the thermodynamic product, since the naked cation in **4c** is solvent stabilized. The backbiting energy, estimated as the energy diffrenece between **4c** and **4b**, decreases from 32 kJ mol^{-1} in the gas phase, to 23 kJ mol^{-1} when solvent effects are considered, confirming that the backbiting of the penultimate unit is not a hinder for the next insertion reaction.

(6) Ti^{II} Species. In this section, we discuss on the possible role that neutral and cationic Ti^{II} species of the type CpTi^{II}P and (arene)Ti^{II}P$^+$, respectively, could have in the syndiospecific polymerization of styrene. The latter is the species proposed to be active with Cp-free based systems. In this case, the Cp ring would be replaced by an arene neutral η^6-ligand, affording a cationic Ti^{II} complex.[34] In the following calculations, we assumed benzene as model for the arene neutral η^6-ligand, and thus the cationic Ti^{II} species will be of the type (C_6H_6)Ti^{II}P$^+$. We then calculated geometry and energy of the most relevant structures of the reaction path. In particular, for both the neutral CpTi^{II}P, and the cationic (C_6H_6)Ti^{II}P$^+$ species we considered the analogues of the monomer-free species **1c**, of the coordination intermediates **2a**, **2c** and **2e**, and of the transition state **3c**. Since we are in the presence of a formal d^2 metal, we considered both low and high-spin species. For these reasons, we labeled these species with a **0** or a +, to denote the charge of the d^2 species, and with a **LS** or a **HS**, to denote the spin state. Thus **1c0-LS** and **1c+-LS** correspond to the low-spin and monomer-free neutral and cationic CpTiCH$_2$Ph and (C_6H_6)TiCH$_2$Ph$^+$ analogues of **1c**. The energies of these structures are reported in Table 2. For the sake of comparison, the results relative to the cationic Ti^{III} d^1 species discussed so far are also reported. Finally, to understand the differences between the Ti^{III} d^1 species and the Ti^{II} d^2 species of low and high spin, we will make reference to the orbitals reported in Figure 7. These are the frontier d-orbitals of the CpTiCH$_2$Ph^{n+} (n = 0, 1) fragment which are involved in the styrene coordination.

Table 2. Calculated Energies of the Most Relevant Structures along the Insertion Reaction Path, for the Cationic CpTi^{III}P$^+$ d^1 Species, for the Neutral Low- and High-Spin CpTi^{II}P d^2 Species, and for the Cationic (C_6H_6)Ti^{II}P$^+$ d^1 Species

	ΔE (kJ mol^{-1})				
		neutral CpTi^{II}P		cationic (C_6H_6)Ti^{II}P$^+$	
species	cationic CpTi^{III}P$^+$ d^1	d^2 low-spin	d^2 high-spin	d^2 low-spin	d^2 high-spin
η^7-chain, + free monomer	0 (**1c**)[a]	0 (29)[b]	0	0 (16)[c]	0
η^7-chain, η^2-monomer	−88 (**2a**)[a]	−87	−9	−58	−21
σ-chain, *trans*-η^4-monomer	−70 (**2c**)[a]	−68	−7	−46	*d*
σ-chain, *cis*-η^4-monomer	−74 (**2e**)[a]	−84	−25	−54	−9
insertion transition state	−41 (**3c**)[a]	+36	+41	+6	+5
barrier to insertion	47	123	50	64	46

[a] The label of the corresponding structure sketched in Figures 1−8. [b] The energy of the neutral CpTi^{II}CH$_2$Ph low-spin structure, with respect to the analogous high-spin species, first row of the next coloumn. [c] The energy of the cationic (C_6H_6)Ti^{II}CH$_2$Ph$^+$ low-spin structure, with respect to the analogous high-spin species, first row of the next coloumn. [d] Converges into σ-chain, cis-η^4 monomer.

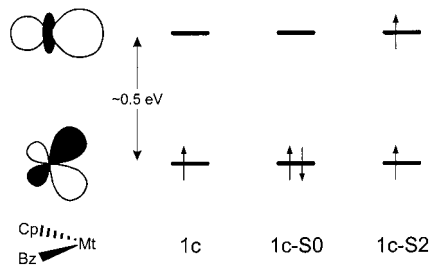

Figure 7. Schematic representation of the frontier d orbitals of the CpTiCH$_2$Ph^{n+} (n = 0, 1) fragment which are involved in styrene coordination.

With regards to the monomer-free species, the high-spin structure is slightly more stable than the low-spin structure both for the CpTi^{II}P and the (C_6H_6)Ti^{II}P$^+$ species (by 29 and 16 kJ mol^{-1}, respectively). Styrene coordination to the monomer free CpTi^{II}P and (C_6H_6)-Ti^{II}P$^+$ species leads to the coordination intermediates **2a0-LS**, **2a0-HS**, and **2a+-LS**, **2a+-HS** of Figure 8, respectively, with the monomer η^2 coordinated. For the case of **2a0-LS** and **2a+-LS**, styrene coordination is exothermic by 87 and 58 kJ mol^{-1}, for the neutral and

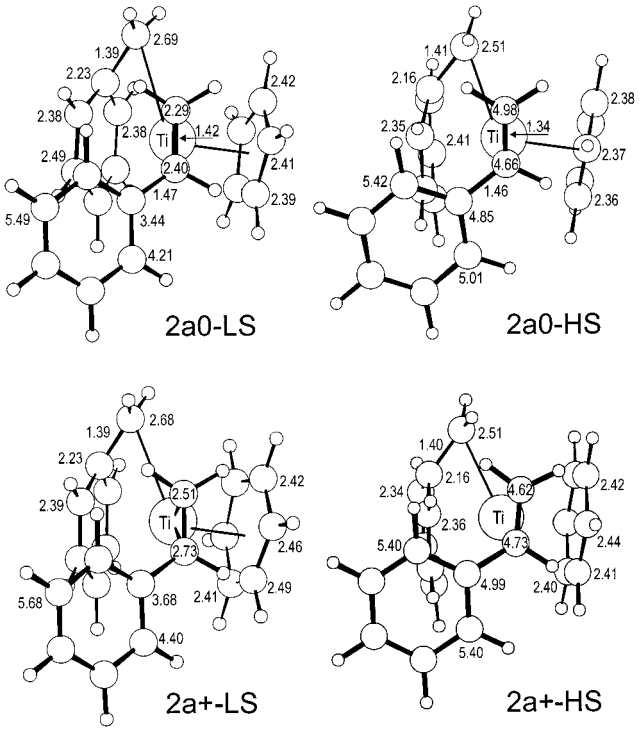

Figure 8. Minimized energy geometries of the most stable low and high-spin coordination intermediates obtained by styrene coordination to the neutral $CpTi^{II}CH_2Ph$, and cationic $(C_6H_6)Ti^{II}CH_2Ph^+$, species. The numbers close to the C atoms represent the distance of these atoms from the metal. All distances are reported in Å.

cationic species, respectively, a value which is comparable to the styrene uptake energy to the corresponding cationic d^1 species **1c**. The high value of the uptake energy for these low-spin species is essentially due to the increased d−π* back-donation which involves a doubly occupied d orbital in the low-spin coordination intermediate (see Figure 7), whereas it involves a singly occupied d orbital in **2a**. The increased back-donation is also suggested by the shorter distances between the metal atom and the olefinic C atoms of the styrene, and by the longer C−C olefinic bond in **2a0-LS**, relative to **2a**. Finally, the reduced uptake energy and the longer metal styrene distances for the cationic species **2a+-LS**, is due to the reduced strength of the d−π* back-donation, which involves d orbitals of the cationic $(C_6H_6)Ti^{II}P^+$ species, which are of lower energy with respect to the d orbitals of the isoelectronic neutral $CpTi^{II}P$ species.

In contrast, styrene coordination to the high-spin structures **1c0-HS** and **1c+-HS**, which leads to the coordination intermediates of **2a0-HS** and **2a+-HS**, shows a very small uptake energy, 9 and 22 kJ mol^{-1} only, for the neutral and cationic species, respectively. The very long distances between the metal atom and the olefinic C atoms of the styrene, are indicative of a very weak interaction between the styrene and the $CpTiCH_2Ph$ or $(C_6H_6)TiCH_2Ph^+$ fragments. The reduced propensity to coordination of the monomer is a consequence of the filling of the orbital of higher energy of the $CpTiCH_2Ph$ or $(C_6H_6)TiCH_2Ph^+$ fragments, which is the metal acceptor orbital for the olefin π−d donation. A similar scheme explains the higher stability of the low-spin intermediates with a η^4-coordinated styrene with respect to the high-spin analogues.

As for the insertion step, both the low- and high-spin transition states are of considerably high energy. In the case of the neutral **3c0-LS** and **3c0-HS** transition states, the calculated barriers with respect to the most stable **2a0-LS** and **2a0-HS** coordination intermediates amount to 123 and 66 kJ mol^{-1}, respectively. The higher barriers calculated for these d^2 species can be easily rationalized in the framework of the studies of Ziegler and co-workers.[48,73] In both **3c0-LS** and **3c0-HS**, the high energy barrier is due to the absence/disruption of the $\pi-\pi$* mixing of the olefin orbitals, which stabilizes the transition state. The reduced involvement of the π* olefin orbital to the stabilization of the transition state is due to its involvement in the d−π* back-donation. Clearly, the higher barrier shown by the low-spin species is in agreement with the stronger back-donation in **2a0-LS** relative to that in **2a0-HS**. A very similar reasoning can be used to rationalize the relative energies we calculated in the case of the cationic **3c+-LS** and **3c+-HS** transition states. The calculated barriers with respect to the most stable **2a+-LS** and **2a+-HS** coordination intermediates amount to 64 and 46 kJ mol^{-1}, respectively.

Moreover, the relatively smaller barrier calculated for the cationic Ti^{III} d^1 species with respect to the high-spin neutral species, (in both of them back-donation involves a singly occupied metal orbital) can be explained by the higher stability of the metal d orbitals in the cationic species with respect to the same orbitals in the neutral species. As a consequence, the energy loss due the reduced back-donation in the transition state is smaller in the cationic than in the neutral species. This analysis is confirmed by the fact that a similar barrier is calculated for the cationic Ti^{III} d^1 species and for the high-spin cationic Ti^{II} d^2 species.

Finally, both transition states for the neutral and cationic d^2 species are higher in energy than the isolated $CpTi^{II}CH_2Ph$, or $(C_6H_6)CpTi^{II}CH_2Ph^+$, and styrene species. In particular, **3c0-LS** and **3c0-HS** are 36 and 41 kJ mol^{-1} higher in energy than **1c0-LS** and **1c0-HS** plus a free styrene molecule, while **3c+-LS** and **3c+-HS** are 6 and 17 kJ mol^{-1} higher in energy than **1c+-LS** and **1c+-HS** plus a free styrene molecule. This is in sharp contrast with respect to the case of the cationic Ti^{III} d^1 species. In fact, in this case **3c** lies 41 kJ mol^{-1} below **1c** plus a free styrene molecule. Moreover, solvent effects previously described, and unfavorable $-T\Delta S$ contributions[63−65] will further destabilize the transition states for Ti^{II} d^2 species with respect to the separate reactants, by roughly 10 and 40 kJ mol^{-1}, respectively.[77] Thus, these calculations suggest that insertion of the coordinated styrene is strongly disfavored with respect to detachment for both the low and high-spin neutral Ti^{II} species, since the corresponding transition states can be estimated to be roughly 75−90 kJ mol^{-1} higher in energy than the separate reactants, if solvent and entropic contributions are considerd. It is difficult for the low- and high-spin cationic Ti^{II} species, since the corresponding transition states are roughly 55−70 kJ mol^{-1} higher in energy than the separate reactants. It is strongly competitive with respect to styrene detachment for the cationic Ti^{III} species, since the corresponding transition state is roughly 10 kJ mol^{-1} higher in energy than the separate reactants also considering unfavorable solvent and entropic contributions. Although not conclusive, these results strongly support the proposal that the active species is of the type

$CpTiP^+$, being III the titanium oxidation state, for Cp-based systems, and they also support the proposal that a species of the type (arene)TiP^+, being II the titanium oxidation state, is the active one for Cp-free systems. Moreover, our findings are in qualitative agreement with the smaller activity of Cp-free systems with respect to Cp-based systems.[33,34,36]

Conclusions

In this paper we have presented a DFT study of a possible mechanism of propagation in the polymerization of styrene with Cp-based and Cp-free catalysts. The main conclusions can be summarized as follows:

(i) The most stable styrene-free $CpTiCH_2Ph^+$ species with a coordinated benzene molecule to simulate the solvent is characterized by a coordination scheme in which the aromatic ring of the last inserted monomeric unit presents a η^3 coordination scheme, with a strong σ-bond between the Ti atom and the C atom of the benzylic CH_2 group. An alternative structure is characterized by a coordination scheme in which the aromatic ring of the last inserted monomeric unit η^7 coordinates to the metal atom with all the C atoms. The η^3 coordination being more stable than the η^7 coordination by 12 kJ mol^{-1}.

(ii) Styrene can coordinate to both monomer-free structures, generating coordination intermediates with different hapticity of coordination. Structures in which the growing chain and the monomer are η^7 and η^2 coordinated, respectively, are slightly more stable than coordination intermediates in which the growing chain and the monomer are η^3 and η^4 coordinated, respectively. Coordination intermediates with different hapticity of coordination of the various ligands can interconvert into each other with small energy barriers. This finding is in agreement with the fluxionality of coordination experimentally observed for the $[Cp^*Ti(CH_2Ph)_2]^+[B(CH_2Ph)C_6F_5)_3]^-$ system.

(iii) The various coordination intermediates can proceed to different transition states for the insertion reaction. However, only the transition state **3c**, reached from the coordination intermediate with a η^4-coordinated monomer and with a relative anti disposition of the Cp ring and of the styrene aromatic ring, is of low energy. The corresponding energy barrier with respect to the most stable coordination intermediate **2a** is 47 kJ mol^{-1}.

(iv) The kinetic product is characterized by a η^3 bonding of the new benzyl-type chain-end, and can interconvert with a small barrier to the thermodynamic product, characterized by a η^7 bonding of the chain-end. Both products present a backbiting of the aromatic ring of the penultimate monomeric unit to the metal atom.

(v) The possible role of neutral d^2 species of the type $CpTi^{II}P$ as active in polymerization is scarcely supported by the present study, since higher energy barriers are found for styrene insertion into the Ti−chain bond of such titanium II species. Even more important, is the fact that the transition states for the insertion reaction with neutral species are quite higher in energy than the monomer-free species plus a free styrene molecule. For the cationic d^1 species, instead, the transition state for the insertion reaction is more stable than the monomer-free species plus a free styrene molecule.

(vi) As for Cp-free catalysts, the possible role of cationic d^2 species of the type (arene)$Ti^{II}P^+$ as active in polymerization is clearly supported by the present study, since energy barriers slightly higher than that evaluated for $CpTi^{III}P^+$ are found. Moreover, the transition states for the insertion reaction with cationic d^2 species are not that higher in energy than the monomer-free species plus a free styrene molecule. Finally, coordination of the monomer is less favored than in the case of $CpTi^{III}P^+$. These findings are in agreement with the reduced activity of Cp-free catalysts when compared to Cp-based catalysts.

Acknowledgment. We thank our colleagues at the University of Salerno for useful discussions. This project has been supported by MURST of Italy, Grants PRIN-1998 and PRIN-2000, and by Montell Polyolefins.

References and Notes

(1) Review: Tomotsu, N.; Ishihara, N.; Newman, T. H.; Malanga, M. T. *J. Mol. Catal. A* **1998**, *128*, 167.
(2) Review: Pellecchia, C.; Grassi, A. *Top. Catal.* **1999**, *7*, 125.
(3) Review: Ewart, S. W.; Baird, M. C. In *Metallocene Based Polyolefins, Preparation, Properties and Technology*; Scheirs, J., Kaminsky, W., Ed.; John Wiley & Sons: New York, 2000; Vol. 1, p 119.
(4) Review: Ewart, S. W.; Baird, M. C. *Top. Catal.* **1999**, *7*, 1.
(5) Review: Po, R.; Cardi, N. *Prog. Polym. Sci.* **1996**, *21*, 47.
(6) Review: Vittoria, V. In *Handbook of Thermoplastics*; Olabisi, O., Ed.; Marcel Dekker: New York, 1997; p 81.
(7) Guerra, G.; Vitagliano, V. M.; De Rosa, C.; Petraccone, V.; Corradini, P. *Macromolecules* **1990**, *23*, 1539.
(8) Ishihara, N.; Seimiya, T.; Kuramoto, M.; Uoi, M. *Macromolecules* **1986**, *19*, 2464.
(9) Ishihara, N.; Kuramoto, M.; Uoi, M. *Macromolecules* **1988**, *21*, 3356.
(10) Zambelli, A.; Pellecchia, C.; Oliva, L.; Han, S. *J. Polym. Sci.* **1988**, *26*, 365.
(11) Chien, J. C. W.; Salajka, Z. *J. Polym. Sci., Part A: Polym. Chem.* **1991**, *29*, 1243.
(12) Chien, J. C. W.; Salajka, Z. *J. Polym. Sci., Part A: Polym. Chem.* **1991**, *29*, 1253.
(13) Kaminsky, W.; Lenk, S. *Macromol. Symp.* **1997**, *118*, 45.
(14) Kaminsky, W.; Lenk, S.; Scholz, V.; Roesky, H. W.; Herzog, A. *Macromolecules* **1997**, *30*, 7647.
(15) Schneider, N.; Prosenc, M.-H.; Brintzinger, H.-H. *J. Organomet. Chem.* **1997**, *545*, 291.
(16) Xu, G. X.; Ruckenstein, E. *J. Polym. Sci., Part A: Polym. Chem.* **1999**, *37*, 2481.
(17) Foster, P.; Chien, J. C. W.; Rausch, M. D. *Organometallics* **1996**, *15*, 2404.
(18) Quyoum, R.; Wang, Q.; Tudoret, M.-J.; Baird, M. C.; Gillis, D. J. *J. Am. Chem. Soc.* **1994**, *116*, 6435.
(19) Pellecchia, C.; Longo, P.; Proto, A.; Zambelli, A. *Makromol. Chem., Rapid. Commun.* **1992**, *13*, 265.
(20) Ammendola, P.; Pellecchia, C.; Longo, P.; Zambelli, A. *Gazz. Chim. Ital.* **1987**, *117*, 65.
(21) Resconi, L.; Cavallo, L.; Fait, A.; Piemontesi, F. *Chem. Rev.* **2000**, *100*, 1253.
(22) Ricci, G.; Bosisio, C.; Porri, L. *Macromol. Rapid. Commun.* **1996**, *17*, 781.
(23) Buschges, U.; Chien, J. C. W. *J. Polym. Sci., Part A: Polym. Chem.* **1989**, *27*, 1525.
(24) Chien, J. C. W.; Salajka, Z.; Dong, S. *Macromolecules* **1992**, *25*, 3199.
(25) Gillis, D. J.; Tudoret, M.-J.; Baird, M. C. *J. Am. Chem. Soc.* **1993**, *115*, 2543.
(26) Kucht, H.; Kucht, A.; Chien, J. C. W.; Rausch, M. D. *Appl. Organomet. Chem.* **1994**, *8*, 393.
(27) Grassi, A.; Pellecchia, C.; Oliva, L.; Laschi, F. *Macromol. Chem. Phys.* **1995**, *196*, 1093.
(28) Grassi, A.; Zambelli, A.; Laschi, F. *Organometallics* **1996**, *15*, 480.
(29) Xu, G.; Lin, S. *Macromolecules* **1997**, *30*, 685.
(30) Grassi, A.; Saccheo, S.; Zambelli, A.; Laschi, F. *Macromolecules* **1998**, *31*, 5588.
(31) Po, R.; Cardi, N.; Abis, L. *Polymer* **1998**, *39*, 959.
(32) Williams, E. F.; Murray, M. C.; Baird, M. C. *Macromolecules* **2000**, *33*, 261.
(33) Grassi, A.; Longo, P.; Proto, A.; Zambelli, A. *Macromolecules* **1989**, *22*, 104.

(34) Zambelli, A.; Pellecchia, C.; Oliva, L.; Longo, P.; Grassi, A. *Makromol. Chem.* **1991**, *192*, 223.
(35) Longo, P.; Proto, A.; Zambelli, A. *Macromol. Chem. Phys.* **1995**, *196*, 3015.
(36) Kaminsky, W.; Park, Y.-W. *Macromol. Rapid Commun.* **1995**, *16*, 343.
(37) Ready, T. E.; Gurge, R.; Chien, J. C. W.; Rausch, M. D. *Organometallics* **1998**, *17*, 5236.
(38) Ewart, S. W.; Sarsfield, M. J.; Jeremic, D.; Tremblay, T. L.; Williams, E. F.; Baird, M. C. *Organometallics* **1998**, *17*, 1502.
(39) Arai, T.; Ohtsu, T.; Suzuki, S. *Book of Abstracts.* 215th ACS National Meeting, Dallas, TX, March 29−April 2 1998; American Chemical Society: Washington, DC, 1998.
(40) Arai, T.; Ohtsu, T.; Suzuki, S. *Polym. Prepr.* **1998**, *39*, 22.
(41) Longo, P.; Grassi, A.; A.; P.; Ammendola, P. *Macromolecules* **1988**, *21*, 24.
(42) Pellecchia, C.; Longo, P.; Grassi, A.; Ammendola, P.; Zambelli, A. *Makromol. Chem., Rapid. Commun.* **1987**, *8*, 277.
(43) Zambelli, A.; Longo, P.; Pellecchia, C.; Grassi, A. *Macromolecules* **1987**, *20*, 2035.
(44) Grassi, A.; Pellecchia, C.; Longo, P.; Zambelli, A. *Gazz. Chim. Ital.* **1987**, *117*, 249.
(45) Zambelli, A.; Pellecchia, C.; Proto, A. *Macromol. Symp.* **1995**, *89*, 373.
(46) Lohrenz, J. C. W.; Woo, T. K.; Ziegler, T. *J. Am. Chem. Soc.* **1995**, *117*, 12793.
(47) Deng, L.; Woo, T. K.; Cavallo, L.; Margl, P. M.; Ziegler, T. *J. Am. Chem. Soc.* **1997**, *119*, 6177.
(48) Margl, P. M.; Deng, L.; Ziegler, T. *J. Am. Chem. Soc.* **1998**, *120*, 5517.
(49) Minieri, G.; Corradini, P.; Guerra, G.; Zambelli, A.; Cavallo, L. Manuscript in preparation.
(50) *ADF 2.3.0 Users Guide*, Vrije Universiteit Amsterdam: Amsterdam, The Netherlands, 1996.
(51) Baerends, E. J.; Ellis, D. E.; Ros, P. *Chem. Phys.* **1973**, *2*, 41.
(52) Versluis, L.; Ziegler, T. *J. Chem. Phys.* **1998**, *88*, 322.
(53) te Velde, G.; Baerends, E. J. *J. Comput. Phys.* **1992**, *99*, 84.
(54) Fonseca Guerra, C.; Snijders, J. G.; te Velde, G.; Baerends, E. J. *Theor. Chem. Acc.* **1998**, *99*, 391.
(55) Vosko, S. H.; Wilk, L.; Nusair, M. *Can. J. Phys.* **1980**, *58*, 1200.
(56) Becke, A. *Phys. Rev. A* **1988**, *38*, 3098.
(57) Perdew, J. P. *Phys. Rev. B* **1986**, *33*, 8822.
(58) Perdew, J. P. *Phys. Rev. B* **1986**, *34*, 7406.
(59) Klamt, A.; Schüürmann, G. *J. Chem. Soc., Perkin Trans. 2* **1993**, 799.
(60) Pye, C. C.; Ziegler, T. *Theor. Chem. Acc.* **1999**, *101*, 396.
(61) Chan, M. S. W.; Vanka, K.; Pye, C. C.; Ziegler, T. *Organometallics* **1999**, *18*, 4624.
(62) *ADF 2000 Users Guide*, Vrije Universiteit Amsterdam: Amsterdam, The Netherlands, 2000.
(63) Rix, F. C.; Brookhart, M.; White, P. S. *J. Am. Chem. Soc.* **1996**, *118*, 4746.
(64) Musaev, D. G.; Froese, R. D. J.; Svensson, M.; Morokuma, K. *J. Am. Chem. Soc.* **1997**, *119*, 367.
(65) Margl, P. M.; Deng, L.; Ziegler, T. *Organometallics* **1998**, *17*, 933.
(66) Guerra, G.; Longo, P.; Corradini, P.; Cavallo, L. *J. Am. Chem. Soc.* **1999**, *121*, 8651.
(67) Longo, P.; Grisi, F.; Guerra, G.; Cavallo, L. *Macromolecules* **2000**, *33*, 4647.
(68) Guy Orpen, A.; Brammer, L.; Allen, F. H.; Kennard, O.; Watson, D. G.; Taylor, R. *J. Chem. Soc., Dalton Trans.* **1989**, S1.
(69) Pellecchia, C.; Immirzi, A.; Pappalardo, D.; Peluso, A. *Organometallics* **1994**, *13*, 3773.
(70) Bassi, I. W.; Allegra, G.; Scordamaglia, R.; Chioccola, G. *J. Am. Chem. Soc.* **1971**, *93*, 3787.
(71) Woo, T. K.; Fan, L.; Ziegler, T. *Organometallics* **1994**, *13*, 2252.
(72) Woo, T. K.; Margl, P. M.; Lohrenz, J. C. W.; Blöchl, P. E.; Ziegler, T. *J. Am. Chem. Soc.* **1996**, *118*, 13021.
(73) Schmid, R.; Ziegler, T. *Organometallics* **2000**, *19*, 2756.
(74) Grassi, A.; Lamberti, C.; Zambelli, A.; Mingozzi, I. *Macromolecules* **1997**, *30*, 1884.
(75) A different view has been adopted for **4b** to stress its similarity to **1c**.
(76) 40 kJ mol^{-1} is the magnitude of the $-T\Delta S$ contribution experimentally[63] and theoretically[64,65] evaluated for olefin coordination at 300 K to Ni and Pd compounds.
(77) 10 kJ mol^{-1} is the magnitude of the stabilization of **1c** plus free styrene with respect to **2a**, due to sovent effects, and discussed in a previous section. As for the magnitude of the $-T\Delta S$ contribution, see ref 76.

MA002162L